

Loughborough University
Institutional Repository

*An experimental study of
electroacoustic crossflow
microfiltration*

This item was submitted to Loughborough University's Institutional Repository by the/an author.

Citation: WAKEMAN, R.J. and TARLETON, E.S., 1991. An experimental study of electroacoustic crossflow microfiltration. Chemical Engineering Research and Design, 69a, pp. 386-397.

Additional Information:

- This article was published in the journal, Chemical Engineering Research and Design [© Institution of Chemical Engineers] and the definitive version is available from: www.icheme.org/archive

Metadata Record: <https://dspace.lboro.ac.uk/2134/5246>

Version: Accepted for publication

Publisher: © Institution of Chemical Engineers

Please cite the published version.

This item was submitted to Loughborough's Institutional Repository (<https://dspace.lboro.ac.uk/>) by the author and is made available under the following Creative Commons Licence conditions.



For the full text of this licence, please go to:
<http://creativecommons.org/licenses/by-nc-nd/2.5/>

AN EXPERIMENTAL STUDY OF ELECTROACOUSTIC CROSSFLOW MICROFILTRATION

R.J. Wakeman and E.S. Tarleton (e.s.tarleton@lboro.ac.uk)
Separation Processes Centre, University of Exeter, Exeter, UK.

ABSTRACT

Results from an experimental study of the effects of the principal process and suspension characteristics on crossflow microfiltration augmented by electrical and ultrasonic force fields are presented. It has been found that both fields, either in isolation or in combination, can reduce membrane fouling: the extent of filtration improvement is affected by field strengths, acoustic frequency, suspension concentration, liquid viscosity, and particle size and surface charge. Synergistic effects were observed when the fields were applied simultaneously. As well as increasing filtrate fluxes, use of either or both force fields allows lower crossflow velocities to be used. This implies that smaller equipment can be used for a given throughput, reduced energy consumption is possible by the recirculation pump, there is a lesser tendency to degrade shear sensitive streams, and heat transfer duties may be reduced for recirculation loop exchangers.

INTRODUCTION

The use of additional forces to aid filtration has been attracting an increasing amount of attention in recent years. Magnetically assisted filters are now widely accepted as technical alternatives in the choice of solid/liquid separation equipment, commercial electrically assisted filters exist but they have not been adopted widely, and ultrasonically assisted filters are found almost exclusively in research laboratories. There is a general understanding of the role of magnetic and electric fields when used to enhance filters, but the same cannot be claimed of ultrasonics where none of the work involving filters has been aimed at providing a reasonable database of information from which some understanding of the underlying phenomena may be gained. This paper is concerned with providing some insight into the use of electric and ultrasonic fields to enhance the performance of crossflow filters.

There is a growing body of work on the use of electrical force fields in filtration¹⁻¹⁵. The earliest attempts to utilise the effects of electric fields were to promote cake dewatering by making use of electroosmotic effects in beds of fine particles, but more recent work related to cake filters has been to enhance the separation by using both electrophoretic and electroosmotic effects to increase filtration rates and to yield a cake with a higher solids content^{1,2,5,6,9}. The industrial take-up of crossflow filtration in the 1980's as a means of slurry dewatering has focussed more recent interest on using the electrophoretic effects to reduce fouling of the filter surface^{3,4,7,8,10-15}. Crossflow filtration was conceived as a means of removing liquid from a suspension rapidly by preventing cake formation at the filter surface. Cake formation was conceived as a means of removing liquid from a suspension rapidly by preventing cake formation at the filter surface. Cake formation was intended to be prevented by using adequate crossflow velocities to induce high shear rates across the filter septum; crossflow velocities of 3 m s^{-1} were quite usual in the earlier days of crossflow filtration, but the failure of the shear generated by these velocities to increase permeate (filtrate) rates has led industry to use increasingly higher crossflow velocities until today when 4 to 7 m s^{-1} is quite usual. In many, if not a majority, of instances these high shear rates do not prevent contamination of the surface and can actually further decrease permeation rates¹⁶.

Various other techniques, including the use of abrasives and filter aids, backwashing and backpulsing, flow reversal and pulsed crossflows have been devised to reduce the effects of the fouling layers. These techniques generally lead to reduced membrane lifetimes or to complexities in the filter operating cycle, both of which are undesirable. Fouling can be reduced progressively by increasing the electric field strength to induce an electrophoretic velocity to the particles in the

feed stream in a direction away from the filter surface. The extent of the increase in permeate rates as a result of imposing the electric field is ultimately dependent on the particle size and the charge density around its surface. Crossflow electrofiltration offers great promise in reducing the fouling problems associated with charged particles and colloids¹²⁻¹⁵, although further efforts are needed to reduce the total power consumed by the filter and there is potential to increase permeate rates over and above those obtained using electrical assistance alone. This aspect is given further consideration in this paper.

Properties and small scale uses of ultrasound have been studied extensively by physicists and others, and as a result macrosonic applications can be found in several areas of industrial process engineering, for example in extraction processes and in cell disruption, atomisation and emulsification, the dispersion of solids, nucleation and growth in crystallisation processes, and for degassing and cleaning. In other areas, including sterilization, flotation, filtration and drying, existing work has been experimental and at the laboratory scale. Approaches to these latter applications of ultrasound have been largely empirical, but increases in filtration rates have been reported with ultrasonically enhanced filtering, where the horn was in direct contact with the filter septum or was placed in the liquid close to the filter¹⁷⁻²⁴. Although these papers refer to filtration, careful analysis of their contents suggests that it is really an acoustic dewatering of the cake to which some actually refer²⁰⁻²³. Reductions of cake moisture can be accomplished more rapidly and to a lower final moisture content using an acoustic field combined with pressure than using pressure alone. In these work²⁰⁻²³ a 20 kHz signal has been applied at 2.5 W cm⁻², whilst in others^{18,19} the same frequency was used at 0.6 to 6 W cm⁻². A filter (referred to as a particle classifier by the inventors) assisted by ultrasonics has been developed for commercial use²⁴, operating continuously at 19 kHz and 300 W. The sonics are used to remove the cake from a rotating metallic filter candle, thereby reducing the cake thickness; this is really an alternative to other techniques of delayed cake formation which are used on conventional cake filters. There do not appear to be any applications of ultrasonics to aid the filtration *per se* apart from the earlier attempts by Semmelink¹⁷ and Fairbanks¹⁸.

The use of combined electrical and ultrasonic fields to aid filtration has been reported by Muralidhara *et al.*^{21,23}; the titles of these works are misleading for it is again cake dewatering that appears to have been studied rather than the filtration process itself. The subject of this paper, electrical and ultrasonic field enhanced crossflow microfiltration, has not been by studied by other workers elsewhere; the combined fields have been used by the authors^{25,26} as a means of reducing fouling in crossflow filters as a natural extension of their previous work utilising electrical fields^{10,12,13}. Initial work²⁵ indicated that use of an ultrasonic field could increase filtration rates under some circumstances, but in as many other instances the effect was to reduce filtration rates; the primary reason for these contradictory results was unclear. Further work²⁶ using a refined technique showed that more intense sound fields increased filtration rates in the absence of electric fields, and that when both were applied simultaneously a synergistic effect resulted in a markedly improved filtration rate. This paper sets out new results from a range of experiments carried out to identify the effects of the main parameters in an augmented crossflow microfiltration system.

EXPERIMENTAL TECHNIQUES AND PROCEDURES

The experimental programme can be conveniently divided into two parts; characterisation tests to provide background knowledge about the properties of the particles, suspensions and membranes used, and crossflow filtration experiments to assess fouling.

Suspension and Membrane Characterisation

The particle size distributions of the test suspensions were evaluated using Malvern Auto- and Master- Sizer instruments. The relationship between pH and particle surface charge was

determined for each suspension using a Malvern Zetasizer. The calcite powder was analar grade supplied by BDH, the anatase was obtained from Tioxide PLC in an uncoated form, and the china clay was supplied by ECC International Ltd. The particles were chosen primarily for their different size, shape and surface charge characteristics, whilst at the same time being representative of 'real' particulates, rather than being idealised such as latex or silica spheres. For each suspension used the size distribution was measured together with the electrophoretic mobility vs. pH relationship.

The membranes were selected to give septa with differing structures and pore size ratings. Their pore size distributions were measured using a Coulter Porometer, and their topography examined using scanning electron microscopy. This confirmed the predominantly cylindrical nature and random dispersity of the pores over the surface of the Nuclepore membrane, and the randomised structure and pore shape associated with the Asypor and Sartorius membranes.

A summary of the main features of the characterisations is given in Table 1.

Fouling Assessment Experiments

The equipment used to assess the membrane fouling behaviour, and hence the effectiveness of the electrical and ultrasonic force fields, is shown schematically in Figure 1. The test rig consisted of a flow loop around which a suspension of known and essentially constant composition was pumped continuously through a crossflow microfilter at a constant crossflow velocity and trans-membrane pressure. The filter was specially designed to include mesh electrodes either side of a planar membrane and ultrasound generators in contact with the suspension on the upstream side of the membrane. The microfiltration membranes used for most of the work were 0.2 μm and 0.8 μm Asypor (mixed esters of cellulose, asymmetric membranes supplied by Domnick Hunter), and fewer experiments were carried out using 0.2 μm Nuclepore (polycarbonate, homogeneous structure) and 0.2 μm Sartorius (cellulose nitrate, homogeneous structure) membranes. The purpose built microfilter was constructed from plastics and stainless steel (as was the rest of the flow circuit and ancillaries) and consisted of a supported 38 cm^2 membrane positioned to form one side of a rectangular flow section. Several interchangeable filter bodies enabled the distance of the ultrasonic transducers from the membrane (equal to the channel height of the filtration cell) to be varied from 15 mm to 100 mm. The ultrasound horns gave a nominal power output of 3 W cm^{-2} and were mounted such that the generated sound waves travelled through the feed suspension to impinge on any surface foulant or deposit which might accumulate on the membrane. Ultrasonic frequencies of 23 and 40 kHz were available. The electric field was applied through the electrodes from a d.c. power supply capable of delivering up to 400 V and 10 A. (Additional electrofiltration experiments (without ultrasonics) were carried out using a similar rig operating at controlled crossflow velocity, trans-membrane pressure, and temperature. The membrane area in this filter was 24 cm^2 .)

Prior to the start of a filtration test the suspension was made up to a known concentration using either dry powder or a slurry added to double distilled water (in a few experiments glycerol/water mixtures were used as the continuous phase), and the resultant mixture was agitated in the feed tank for several minutes to produce an homogeneous mixture. The suspension pH was then altered to the required value using NaOH or HCl. No other dispersants or flocculants were added. The test was then performed at the desired filtration conditions. The filtrate produced was collected via porting behind the membrane; its flow rate was measured continuously and its clarity checked visually before it was returned to the feed tank. In all of the experiments reported a visually clear filtrate was produced. The temperature of the suspension was maintained at approximately 25°C during each test.

A systematic experimental programme was followed to examine effects of the matrix of parameters shown on Table 2.

RESULTS AND INTERPRETATION

The results from this work fall naturally into three sections: the first presents new data on the effects of electric fields on crossflow filter performance and supplements previously published results^{8,10,12-15}; the second gives original information on the effects of an ultrasonic field on crossflow filtration, in the absence of an electric field; and the third part presents original data on the combined effects of electric and ultrasonic fields on crossflow filtration. The latter problem does not appear to have been studied previously, and the data point to results which may have considerable industrial significance. Measurements were taken with feed suspensions carrying solids in the range 0.01 to 5% by volume; for convenience these are converted into % by mass in Table 3, from where it can be seen that low to high mass fraction feeds have been used.

(i) Effects of an Electric Field Gradient in the Absence of an Ultrasonic Field

Figure 2 shows the influence of a DC electric field on the filtrate flux during crossflow filtration of anatase suspensions; these results confirm the form of data measured previously^{7,10,12-15}. In the experiments shown equilibrium flux increases of x4, x9, and x14 were observed on the application of electric field gradients of 25, 50 and 100 V cm⁻¹ respectively, with no loss of filtrate clarity. The extent of flux improvement is dependent primarily on particle size and surface charge and on the magnitude of the imposed field gradient. Greater flux enhancements are possible for finer particles carrying higher surface charges, and when using steeper field gradients. The field gradient is dependent on the applied voltage and the inter-electrode distance, and clearly electric power consumption can be reduced by designing the separation distance to be as small as possible. Gas evolution by electrolysis occurred in all experiments. The problem of membrane fouling by gas bubbles had been identified in earlier work^{10,12,13} and was overcome by having one electrode downstream of the membrane support, so that bubbles were carried away with the filtrate flow. The other electrode could not be placed closer than about 3 mm from the membrane surface, and gas evolved from this electrode was flushed out of the filter by the crossflow stream.

A further way to reduce power input to the filter would be to reduce the crossflow velocity; it has already been noted that high crossflows do not guarantee a reduction of fouling. When an electric field is used a lower crossflow velocity can be a positive advantage, particularly when the particle charge is close to the isoelectric point. This is demonstrated on Figure 3. At low ζ -potentials and high crossflow velocities there is no improvement in the equilibrium (or more strictly pseudo-equilibrium) flux, but by reducing the crossflow velocity (and thereby increasing the residence time of the particles in the filter) a considerable flux improvement is possible when an electric field is applied.

The mechanisms of enhancement are recognised as being due to electrophoresis with electroosmosis as a secondary electrokinetic phenomenon. However, what is significant in an industrial context is that low crossflow velocities may be useable, contrary to the current thinking on the operation of conventional crossflow microfilters. Further investigation of this point showed that crossflow velocities of 0.1 m s⁻¹ could be used to advantage. In subsequent work using the ultrasonic fields 0.1 m s⁻¹ was used (this velocity is over an order of magnitude less than that commonly used in industrial crossflow filters). This offers potential advantages in terms of reduced pumping costs, less heat input into the process stream, and the improved possibilities of processing shear sensitive streams, albeit at the expense of the energy input required to generate the electric field.

(ii) Effects of an Ultrasonic Field in the Absence of an Electric Field

There is no literature data pertaining to the use of ultrasound as an aid to crossflow filtration, but its use in other areas of processing has produced results which it was thought would have some relevance to this work. High energy ultrasound at lower frequencies (20 to 100 kHz) produces an

effect on the medium through which it is propagated, and has been used for ultrasonic cleaning, modifying chemical reactions, emulsification, and so on. The observable effects are the results of three main phenomena: cavitation, rapid movement of fluids caused by variation of sonic pressure, and microstreaming. Investigations of cavitation mechanisms are linked to measurements of cavitation thresholds; the threshold for rectified diffusion is the acoustic pressure at which bubbles oscillating around some equilibrium radius start to grow by rectified diffusion, and the transient cavitation threshold is the value of the acoustic pressure necessary for the cavity to expand in an unstable fashion. From the point of view of the present work the transient cavitation threshold is taken to be the value of the acoustic pressure at which a change in the filtration characteristics is detected. Even though this threshold may be defined differently from that used in ultrasonics work, it is anticipated that both will vary in similar way as functions of various liquid properties. General observations of the effects of liquid properties on the transient cavitation threshold have been compiled from the results of reported research²⁷ and can be summarised as in Table 4.

If nuclei are found to aid membrane filtration it is recognised that they may be different in behaviour from those formed in a large stagnant volume, as the environment in which the bubbles are formed can affect their behaviour. For example, a streaming behaviour with little coalescence of the bubbles may be observed in a large liquid volume but in a filter streaming is likely to be followed by rapid coalescence due to the constrained height in which the liquid volume is contained.

(a) Ultrasonic Frequency and Field Strength

Figure 4 shows the effect of ultrasonic frequency on permeate flux. The greater flux improvements with a 23 kHz sound field suggests that cavitation is going to be an important factor, when a more vigorous 'surface cleaning' action and less sound absorption by particulate matter would be expected. In the light of the information shown on Figure 4 and by other similar data all further experiments were carried out at a frequency of 23 kHz.

The intensity of the sound field is expressed in this work as the ultrasonic power density gradient ($\text{W cm}^{-2} \text{ cm}^{-1}$). The gradient was varied by using an ultrasonic source with a fixed power output and changing its separation distance from the membrane surface. Some typical results are shown on Figure 5, where it is seen that as the source is brought closer to the membrane the effect of the ultrasound on improving filtration rates increases considerably.

(b) Crossflow Velocity

The results from a number of tests at crossflow velocities between 0.1 and 2.3 m s^{-1} showed that the improvement of filtrate flux by changing velocity alone is small compared with the improvements possible by utilisation of electric or (in many cases) ultrasonic force fields, and that increasing the crossflow velocity does not always lead to an increase in the filtrate flux. Since the small flux improvement is at the expense of a relatively large power input to the recirculation pump it was decided to use a crossflow velocity of 0.1 m s^{-1} for most of the experimentation.

(c) Suspension Concentration

Increasing the suspension concentration was found to reduce the filtration rate enhancements possible with an ultrasonic field. The percentage gain in the filtrate flux as a result of using ultrasound is plotted on Figure 6 as a function of the volume fraction of solids in the feed and the filtration time. The data on Figure 6 shows the typically observed effect of the flux improvement increasing at longer filtration times; it seems that this is because ultrasound causes the deposit thickness to equilibrate more rapidly, leading to a constant flux being achieved sooner than is the case when no ultrasound is used. However, it must also be noted that a higher particle concentration produces greater attenuation of the sound waves as they pass through the crossflow suspension due to increased acoustic impedance. The degree of attenuation varied with different

feed solids and experimental conditions, and is considered to be an important parameter controlling the efficacy of the ultrasonic field.

(d) Liquid Viscosity

Several tests were carried out with glycerol-water mixtures in order to test the hypothesis that any ultrasonic effect would be reduced as the viscosity was increased; this was found to be the case, and attenuation of the sound was effectively total at a suspension viscosity of 4 cp for 1% v/v china clay suspensions. Figure 7 shows the percentage gain in filtration rate after filtering for 60 mins. as a result of using ultrasound plotted as a function of the suspension viscosity; at higher viscosities the gain was constant throughout the filtration test, but at lower viscosities the gain was time dependent. The 2.2 cp data indicated on Figure 7 showed a 23% gain after 1 min. filtration, 80% after 30 mins., and 105% after 60 mins.

(e) Particle Size

The effect of particle size is shown on Figure 8, where data for unground (8 μm) and wet ground (3 μm) calcite suspensions are compared. At the smaller particle size the filtration flux is enhanced by ultrasound, suggesting that less fouling had occurred at the membrane surface. With a smaller mean size the particle movement in the sound field could reasonably be expected to follow more closely that of the suspending fluid, and the ultrasonic field could possibly promote sufficient motion at or near the fouling layer surface to cause the particles to stay in suspension or to resuspend. Alternatively, smaller particles in suspension may cause less attenuation of the sound field. It has to be noted, however, that the situation may be complicated by the substantial increase in the number of cavitation nucleation sites generated on the new particle surfaces by the grinding process. Thus, although the influences of particle size are obviously important no clear operating mechanism can be identified.

Figure 8 shows that ultrasound creates more rapid fouling when larger particles exist in the feed. A possible explanation here is that the momentum needed to resuspend the particles is more than that which can be supplied by the motion of the bubbles resulting from cavitation. However, the bubbles probably cause agitation of the foulant layer and help it to pack more densely and therefore lead to a lower filtrate flux.

(iii) Effects of Combined Electric and Ultrasonic Fields

The effect of surface charge was investigated by altering the suspension pH, and was carried out for anatase and china clay suspensions. For the china clay suspensions the zero charge point occurs at a pH which is so low as to prevent experiments being carried out without disintegration of the membrane by the combined effects of the acidic solution and the ultrasonic field. In the case of anatase the isoelectric charge point is at about pH ~ 4 , where there appeared to be no attack of the membrane. Figure 9 shows the effects of surface charge and the combined electric and ultrasonic fields on filtrate fluxes when filtering anatase suspensions. When no fields are used the flux is similar at both the pH's shown, and in both cases addition of the two force fields causes substantial increases in filtration rates. At a higher ζ -potential the particles are better dispersed, and a greater improvement in filtration rate is measured.

In normal crossflow microfiltration the effect of membrane type appears to be minimal at higher feed concentrations and when the particle size is larger than the pore size of the membrane; this is shown also by the bottom two curves on Figure 10 which were obtained using polycarbonate (Nuclepore) and cellulose nitrate (Sartorius) membranes. In both cases the filtrate flux was markedly increased by the simultaneous addition of electric and ultrasound fields, and from this work there is no evidence that membranes of differing structure will respond differently in either electric, ultrasonic or combined fields.

The contributions of each field to a combined field filtration are shown in Figures 11 and 12. Both electrical and ultrasonic fields are seen to reduce fouling when applied individually, but the extent of improvement by the ultrasonic field can be minimal; this is the case on Figures 11 and 12. The improvement by the electric field is invariably considerably greater than that due to the ultrasonic field, particularly when the particles are well dispersed (high ζ -potential). Comparisons of the effects of the electric fields on Figures 11 and 12 show up marked differences in the early stages of filtration. On Figure 11 the approach to a pseudo-equilibrium flux is quite orderly, with a progressive fouling of the membrane occurring until equilibrium is reached; this is typical of lower concentration feed suspensions. On Figure 12 there is an initial sharp drop in the filtrate flux due to the high initial flux through the clean membrane causing deposition of a cake. The large number of particles approaching the membrane surface cause most of the pores to be bridged and the flow resistance is simply due to cake thickness. The cake is subsequently largely removed by the electric field, and the filtrate flux rises. Once most of the cake has been removed finer particles then start to penetrate the membrane surface and cause the flux to decline; the behaviour of the electric field shown on Figure 12 is typical of higher concentration feeds. When the two fields are applied simultaneously the filtrate flux was significantly better than the additive effects of the individual fields. There is synergy between the electric and ultrasonic fields in all of the data obtained in this work, the synergism being greater with the more problematic suspensions and in particular at higher feed concentrations (for instance, Figure 12 was measured for a 10.1% by mass feed suspension).

DISCUSSION

In crossflow microfiltration the bulk flow is tangential to the membrane where there is also a convective flow into the porous surface which causes particles to be transported laterally toward the membrane. The convective flow of the particles can be counterbalanced to a greater or lesser extent by giving an electrophoretic velocity to the particles through the application of a d.c. electric field gradient. The contribution of fine particles and colloids to membrane fouling can be reduced by this means; the filtrate flux tends to be enhanced more when the feed concentration is lower and the trans-membrane pressure is smaller. An acceptable filtrate flux level from a microfilter would be about $1 \text{ m}^3 \text{ m}^{-2} \text{ h}^{-1}$ (this is rarely achieved and instances of filters operating at lower fluxes are not infrequent, and on most processes $0.5 \text{ m}^3 \text{ m}^{-2} \text{ h}^{-1}$ would be met with unbounded delight). The successful application of electrical assistance would require that an electrophoretic velocity greater than this could be imparted to the suspended matter; the electrophoretic velocity gained by a particle may be estimated from solutions of the Stokes equations subject to the constraints that the velocity in the liquid tends to zero from the particle surface, and that the net force on the particles is zero. One such solution to these equations is the Henry formula which is

$$v \approx \frac{2\varepsilon_0 D \zeta E}{3\mu} \quad (1)$$

Assuming the double layer thickness to be of the same order as the particle radius (this assumption is not important in an order of magnitude calculation, since when the double layer thickness is much less than the particle radius the constants in equation (1) change from 2/3 to 1. If we further assume the suspension to be aqueous and substituting appropriate values into equation (1) (permittivity of a vacuum $\varepsilon_0 = 8.854 \times 10^{-12} \text{ C}^2 \text{ J}^{-1} \text{ m}^{-1}$, dielectric constant $D = 80$, and fluid viscosity $\mu = 10^{-3} \text{ Pa s}$) relates the particle velocity to the imposed field gradient (E) and the zeta potential (ζ) on the particles:

$$v \approx 4.722 \times 10^{-7} \zeta E \quad (2)$$

Hence, to prevent a particle moving towards the membrane surface a field gradient of

$$E > 588/\zeta \text{ V m}^{-1}$$

is required. This points to the importance of surface charge in electrically assisted microfiltration and gives an idea of the order of magnitude of the parameters involved. It is recognised that this simple analysis assumes that the particles are flowing normal to the membrane surface as they approach it and that all particles in suspension have identical surface properties; neither is true in reality, and the field gradient actually required may be of the order of only 10 to 20% of the calculated value. In experiments the same general trend is found as that which is suggested by equation (1).

The passage of ultrasound waves through a suspension can cause many phenomena, including particulate dispersion, viscosity reduction, changes in particle surface properties and cavitation. Although dispersion, which could potentially increase fouling due to the formation of higher resistance membrane deposits, was observed with all the feed suspensions tested (particle size distributions in the suspension were monitored during the course of each experiment) it was clear that the combination of cavitation and relative movement between the solid and liquid phases in conjunction with the action of the crossflow stream was responsible for the enhancements observed.

Power ultrasound is characterised by its ability to transmit substantial amounts of mechanical power at small mechanical movements, and primary vibratory inputs from the ultrasonic transducer lead to the occurrence of compound acoustic phenomena. It is known that acoustic pressure causes cavitation and microstreaming in liquids, vibratory stress causes heating and fatigue in solids, and ultrasonic acceleration is responsible for surface instabilities at fluid-fluid interfaces. Vapour bubbles driven by sound fields cool slightly and take in heat from the surrounding fluid on the expansion part of the cycle, and on compression the reverse occurs. Since the expanding area is slightly greater than the contracting area, the bubble gains some heat over a complete cycle. Not only will the increased temperature of the bubble mean that its saturation vapour pressure is increased so that evaporation of liquid to vapour must occur to restore equilibrium, but if the bubble is attached to or very close to the surface of a particle a local change of temperature and ionic composition will occur around the 'double layer' at the particle surface. Therefore we might assume also that the acceleration may cause property changes at fluid-solid interfaces. A 23 kHz transducer operating at a peak displacement amplitude of 50 μm has a peak velocity of $\sim 6 \text{ m s}^{-1}$ and a peak acceleration of $\sim 9 \times 10^4 \text{ g}$. The peak velocity is therefore $\sim 10^5$ greater than the filtrate velocity ($\sim 10^{-1} \text{ mm s}^{-1}$) or the approximate approach velocity of the particles to the membrane surface. Thus both peak velocity and peak acceleration at the transducer surface are very large compared with the fluid and particle velocities and accelerations at the membrane surface.

The difference in the acoustic impedance of the solid and liquid phases in the suspension causes high inertial and elastic forces to be generated at their interfaces, which in turn produces phenomena such as particulate dispersion and cavitation. The latter phenomenon is recognised as being initiated from nucleation sites present as 'free' microbubbles in the carrier liquid, gas pockets on/within suspended particle surfaces and gas pockets at vessel walls (in this case membrane pores). The rapid growth, oscillation and destruction of these gaseous areas, particularly at or near the membrane pore throats and within the fouling layer, are likely to loosen some of the particles forming the fouling layer. It is estimated that a particle displacement of between 1 and 4 μm is needed to move the particles to more favourable positions where the crossflowing stream can re-entrain them. If this is so then increasing the strength of the ultrasonic field would further reduce fouling. Figure 5 shows how moving the ultrasound source nearer to the membrane surface, thereby effectively increasing the strength of the sound waves at the membrane due to reduced attenuation, produces such an effect. Superimposing the electric field on the system means that the particle displacement can be less before re-entrainment occurs, contributing to the synergy shown in Figures 11 and 12.

The experimental results obtained with ultrasound suggest that the mechanisms of sound transport through the feed, the interactions between the ultrasound/feed constituents/membrane and the sound field strength at the filtering surface are of paramount importance. A rigorous theoretical analysis of the processes occurring would be inherently extremely complex, but some explanation of the principles is provided by basic reference works on the absorption of sound in suspensions²⁸⁻³². The motion of a two dimensional sound wave through a suspension of elastic modulus K and density ρ is described by the wave equation

$$\frac{\partial^2 \varepsilon}{\partial t^2} = \left(\frac{K}{\rho} \right) \frac{\partial^2 \varepsilon}{\partial r^2} \quad (3)$$

where ε is the wave displacement. When viscosity and/or particulate matter is present in the suspension the sound waves are attenuated as they pass through the medium and the sound intensity is related to the depth of penetration (x) by

$$I_x = I_0 \exp(-\alpha x) \quad (4)$$

where α is the intensity absorption coefficient and I_0 the ultrasound source strength. The absorption coefficient (α) has been shown²⁹ to be calculable for dilute (< 10% v/v) kaolin and sand suspensions by

$$\alpha = C \left(\frac{k^4 a^3}{6} + \frac{sk(\sigma - 1)^2}{S^2 + (\sigma + \tau)^2} \right) \quad (5)$$

where

$$S = \frac{9}{4\beta a} \left(1 + \frac{1}{\beta a} \right) \quad (6)$$

$$\tau = 0.5 + \frac{9}{4\beta a} \quad (7)$$

$$k = \frac{2\pi f}{c} \quad (8)$$

$$\beta = \sqrt{\frac{2\pi\rho}{\mu}} \quad (9)$$

and a is the particle radius, C the volume fraction of solids in the suspension, f the ultrasound frequency, c the ultrasound velocity through the suspension, μ the dynamic viscosity of the suspending fluid and σ the ratio of particle to fluid densities. Intensity absorption coefficients calculated from equation (5) for the solids and range of suspension concentrations used in this work are given in Table 5. On Table 5 it can be seen that the intensity absorption coefficient α is raised by increasing the solids concentration in the suspension or by increasing the size of the particles; the ultrasound intensities at any distance from the source are correspondingly reduced (see equation (4)). This trend confirms the experimentally determined results.

The values of α given by equation (5) and on Table 5 are strictly only valid for spherical, non-interacting particles in the presence of a non-cavitating sound field. Whilst the former assumptions are reasonable approximations, in the experiments performed it appeared that both 'stable' and

'transient' cavitation bubbles were present. To accommodate the effects of cavitation the theory is modified below to estimate an overall attenuation coefficient which accounts for sound attenuation due both to particle absorption and to cavitation by combining some experimental results with a modified version of equation (4). If it is assumed that the flux improvement ($\varphi - \varphi_0$) as a result of using ultrasound is proportional to the sound intensity at the membrane surface (the corresponding assumption for electrofiltration where flux improvement is proportional to the applied electric field gradient has been found to be true over a range of field strengths¹³, also indicated by Figure 2) then we can write

$$\varphi - \varphi_0 = k_p I_0 \exp(-\alpha x_s) \quad (10)$$

where k_p is a constant of proportionality, x_s the distance between the sound source and membrane and φ_0 the flux recorded in filtration with no imposed force fields. Thus, plotting $\ln(\varphi - \varphi_0)$ vs. x_s for a number of similar experiments with different source-membrane distances should yield a straight line plot. Such plots were possible for a limited number of experiments, from which α values of 19.7 m^{-1} for 0.67% anatase, 29 m^{-1} for 0.57% china clay, and 130 m^{-1} for 1.7% china clay were obtained. Whilst it is recognised that the theory is not rigorous the fact that the attenuation coefficient calculated here is significantly higher than that given by equation (5) suggests that cavitation is present in the system during filtration, and that cavitation substantially contributes to the processes occurring. (It should be noted that even a small amount of cavitation can be very detrimental to sound transmission efficiency and this could easily account for the difference between the values of α calculated by equations (5) and (10)).

To provide some insight into the synergistic effects shown on Figures 11 and 12 it is necessary to consider some details of the likely mechanistic phenomena occurring close to the pore entrances. The form of the electric field gradients at the pore entrances is complex, particularly when the pores are non-cylindrical and possess the ability to surface conduct. Preliminary analysis of the field gradients using finite difference techniques suggests that, under these conditions, the field gradient is lower at the pore entrance than it is above the areas between the pores. The differences between gradients can be substantial, leading to the slower removal of particles from the entrance regions. It is possible that removal is so hindered that particles become effectively trapped around the pore entrances. This is the subject of a continuing study.

The effect of ultrasound is likely to be the generation of bubbles, whether they originate from sites at the membrane or particle surfaces or from gas in solution; in the experiments the water was distilled but not deaerated, hence air bubbles are likely to be formed both in the suspension and at nucleation sites when ultrasound is applied. At pressures of ~ 1 bar streamers of bubbles are formed by rectified diffusion and the equilibrium bubble diameter is $\approx 20 \text{ }\mu\text{m}$ if the bubble cycle is isothermal²⁷ or $\approx 80 \text{ }\mu\text{m}$ if the cycle is adiabatic. A smaller radius is associated with a lower acoustic pressure threshold, largely because as the bubble grows toward resonance size its pulsation amplitude increases which results in more rectified mass transfer per cycle. Hindrance of bubble motion close to the entrance of a pore by the presence of large numbers of particles at a fairly high concentration may cause rapid coalescence of the bubbles, thus increasing their buoyancy and their ability to disturb particles deposited at the membrane surface. Flow oscillations at the membrane surface, together with acoustic streaming, will further enhance rates of bubble growth and coalescence. For the bubble to be buoyant at the surface it has to move against the permeate flux: Stokes Law suggests that the unbounded velocity of a $22 \text{ }\mu\text{m}$ bubble will rise against a permeate flux 1 m h^{-1} , and a $36 \text{ }\mu\text{m}$ bubble against a flux of 2.5 m h^{-1} . These various factors, together with the conditions used in the experiments and the typical results shown in Figures 4 to 12, suggest that bubble streamers formed by rectified diffusion provide for filtration enhancement by ultrasonics. Furthermore, when the ultrasonics is used in combination with the electric field the bubbles have the ability to displace the particles far enough, between 1 and $4 \text{ }\mu\text{m}$, toward the mainstream flow where electrophoresis can then takeover and move them into the bulk of the crossflowing stream.

Power Consumption vs. Process Rate

To increase the filtration rate is not necessarily a sufficient criterion to assess filter performance, but the energy consumed in achieving that rate can be equally as important. There is probably an optimum, which is specific to each filter application, between increasing the rate of separation and the added expenditure on energy. It is pertinent here to point out some general trends. Power consumptions have been monitored for a range of filtration conditions; some values are shown on Table 6. The power to the filter cycle is broken down to show the contributions from the different sources, the pump, the d.c. field and the ultrasonics, and is indicated as power per unit filter area and as energy consumed per unit volume of filtrate. The latter is the more appropriate to consider here as it takes account of the differing filtrate volume fluxes. The first two lines show the value of reducing the crossflow velocity; the pH and ionic strength of the suspension were high to provide well dispersed particles. The improvement of the flux by increasing the crossflow velocity is minimal. It is recognised that the power consumed at 2.3 m s^{-1} is high in comparison with industrial filter units, which more typically have power consumptions³³ in the region of 5 to 12 kW h m^{-3} . It is appropriate only to compare values shown in Table 6 and not to make comparisons between these data and any obtained from elsewhere. However, these industrial energy consumptions could also be lowered considerably by operating at lower crossflow velocities.

The next three rows of data are from a set of three consistent experiments with a fairly high ionic strength in solution, this is reflected in the very high energy consumption by the electric field (93.9 and $124.7 \text{ kW h m}^{-2}$). This energy can be reduced from 132.2 to 33.9 kW h m^{-3} by the addition of an ultrasonic field; although the total energy consumption has been increased when compared with the simple crossflow filter arrangement, it is worth noting that the time taken to produce 1 m^3 of filtrate from a 1 m^2 filter has been reduced from 8.3 h in the simple crossflow mode to 1.4 h when an electric field is used to 0.23 h when the combined fields are used.

The final three rows of data are for another consistent set of experiments with a lower ionic strength in solution, leading to lower energy consumption by the d.c. field. In this instance the electric field had a greater effect on increasing the filtrate rate, and combining this with the ultrasonic power served to increase the energy consumption further.

In this work no attempts have been made to design a filter to consume a minimum of power, either by the imposed electric field or by the ultrasonic field. In the light of supplementary work carried out alongside this project it is considered that the energy consumed by the electric field could be reduced by 25 to 30% , and that consumed by the ultrasonic field by 50 to 60% . This would reduce power input levels to between one half and two-thirds of those shown on Table 6 whilst retaining the filtrate rates shown on the Table; if this proves to be achievable the process may compare favourably with conventional crossflow filtration, particularly for difficult-to-filter or 'high value' suspensions.

CONCLUSIONS

The conclusions to be drawn from this work are several and can be summarised as follows:-

1. Both electric and acoustic fields can reduce membrane fouling caused by the deposition of colloidal material over a range of operating conditions.
2. Flux levels recorded during filtrations assisted by electric and/or ultrasonic fields can be over an order of magnitude higher than corresponding tests with no imposed force fields.

3. The rate of fouling in an electroacoustic filter is affected by parameters such as electric field strength, acoustic field strength and frequency, suspension concentration, particle size, particle shape and the surface properties of the dispersed phase.
4. Electric fields enhance filtration by electrophoresis and other secondary electrokinetic effects such as electroosmosis. Ultrasonic fields cause phenomena such as particulate dispersion, viscosity reduction, changes in particle surface properties and cavitation in suspensions. It seems that filtration is enhanced with acoustic fields largely as a result of cavitation.
5. Synergistic effects can be observed when electric and acoustic fields are applied simultaneously during filtration. The coupling mechanism is believed to be due to a combination of cavitation and electrokinetic effects.
6. Lower crossflow velocities can be used when combined electric and acoustic fields are used to assist filtration. The crossflow velocity used can be an order of magnitude lower than that found in conventional crossflow filtration.
7. Using assisted filtration in conjunction with low crossflow velocities offers the potential advantage of reduced pumping costs, lesser degradation of shear sensitive streams, and reduced heat transfer requirements in batch recirculation systems.

The general effect of the suspension and process properties are summarised in the Table 7. From this Table it may be deduced, in general terms, that electroacoustic augmentation of microfiltration is most effective for feed suspensions containing small particles which are well dispersed (that is, not aggregated) in a liquid which has a viscosity somewhat less than 10 cp. In terms of the filtration parameters, the filter design should accommodate an ultrasound source with a frequency of 23 kHz and both sonic and electric field strengths should be as high as possible. Some feed conditions lead to serious degradation of polymer membranes; it is thought that this is due to a local heating effect at the membrane surface which does not always manifest itself in the bulk of the suspension. To overcome this consideration should be given to the use of membranes made of alternative materials such as ceramics, but for specific applications these would need to be designed to prevent ion dissolution in the electric and ultrasonic fields.

ACKNOWLEDGEMENTS

The authors wish to acknowledge receipt of grants from the Specially Promoted Programme in Particulate Technology of The Science and Engineering Research Council in support of this work, and of additional support from the company members of the Separation Processes Centre at Exeter University.

NOMENCLATURE

a	particle radius (m)
C	volume fraction of solids in suspension
D	dielectric constant
E	electric field gradient ($V\ m^{-1}$)
I_0	ultrasound source strength ($W\ m^{-2}$)
I_x	ultrasound strength at distance x from the source ($W\ m^{-2}$)
k_p	proportionality constant in equation (10) ($m^3\ m^{-2}\ s^{-1}$) ($W\ m^{-2}$) ⁻¹
K	elastic modulus of the suspension ($N\ m^{-2}$)
r	distance coordinate (m)
t	time (s)
v	electrophoretic velocity of a particle ($m\ s^{-1}$)

x	penetration depth of a sound wave (m)
x_s	distance from the sound source to the membrane (m)

Greek letters

α	sound intensity absorption coefficient (m^{-1})
ε	displacement of a sound wave
ε_0	permittivity of a vacuum ($\text{C}^2 \text{J}^{-1} \text{m}^{-1}$)
ζ	zeta potential (V)
μ	liquid viscosity (Pa s)
ρ	density of the suspension (kg m^{-3})
σ	ratio of the particle to fluid densities
φ	permeate (or filtrate) flux ($\text{m}^3 \text{m}^{-2} \text{s}^{-1}$)

REFERENCES

1. S.P. Moulik, F.C. Cooper and M. Bier, 1967, Forced-flow electrophoretic filtration of clay suspensions, *J. Coll. Int. Sci.*, **24**, 427.
2. H. Yukawa, K. Kobayashi, Y. Tsukui, S. Yamano and M. Iwata, 1976, Analysis of batch electrokinetic filtration, *J. Chem. Eng. Japan*, **9**(5), 396.
3. J.D. Henry, L.F. Lawler and C.H.A. Kuo, 1977, A solid/liquid separation process based on crossflow and electrofiltration, *AIChEJ*, **23**(6), 851.
4. C.H. Lee, D. Gidaspow and D.T. Wasan, 1980, Cross-flow electrofilter for nonaqueous slurries, *Ind. Eng. Chem. Fundam.*, **19**, 166.
5. H. Yukawa, K. Kobayashi and M. Hakoda, 1980, Study on performance of electrokinetic filtration using rotary drum vacuum filter, *J. Chem. Eng. Japan*, **13**(5), 390.
6. R.J. Wakeman, 1982, Effects of solids concentration and pH on electrofiltration, *Filt. & Sep.*, **19**(4), 316.
7. J.A. Mikhlin, M.E. Weber and A.K. Turkson, 1982, Electrically aided axial filtration, *J. Separ. Proc. Technol.*, **3**(1), 16.
8. H. Yukawa, K. Shimura, A. Suda and A. Maniwa, 1983, Cross flow electro-ultrafiltration for colloidal solutions of protein, *J. Chem. Eng. Japan*, **16**(4), 305.
9. J.M. Bollinger and R.A. Adams, 1984, Electrofiltration of ultrafine aqueous dispersions, *CEP*, **80**, 54.
10. R.J. Wakeman and E.S. Tarleton, 1986, Experiments using electricity to prevent fouling in membrane filtration, *Filt. & Sep.*, **23**(3), 174.
11. B.M. Verdegan, 1986, Crossflow electrofiltration of petroleum oils, *Sep. Sci. Technol.*, **21**(6 & 7), 603.
12. R.J. Wakeman and E.S. Tarleton, 1986, Membrane fouling prevention in crossflow microfiltration by the use of electric fields, *Chem. Eng. Sci.*, **42**, 829.
13. E.S. Tarleton and R.J. Wakeman, 1988, Prevention of flux decline in electrical microfiltration, *Drying Technol.*, **6**(3), 547.

14. C. Visvanathan and R. Ben Aim, 1989, Application of an electric field for the reduction of particle and colloidal membrane fouling in crossflow microfiltration, *Sep. Sci. Technol.*, **24**(5 & 6), 383.
15. C. Visvanathan and R. Ben Aim, 1989, Application of cross-flow electro-microfiltration in chromium wastewater treatment, *Desalination*, **71**, 265.
16. R.J. Wakeman and E.S. Tarleton, 1991, Colloidal fouling of microfiltration membranes during the treatment of aqueous feed streams, *Desalination*, **83**, 35-52.
17. A. Semmelink, 1973, Ultrasonically enhanced liquid filtering, *Proc. Ultrasonics Symposium*, pp.7-10, IPC Science & Technology Press, Guildford.
18. H.V. Fairbanks, 1973, Use of ultrasound to increase filtration rate, *Proc. Ultrasonics Symposium*, pp.11-15, IPC Science & Technology Press, Guildford.
19. H.V. Fairbanks, W. Morton and J. Wallis, 1986, Separation processes aided by ultrasound, *Proc. 4th World Filtration Congress*, pp.15.1-15.3, KIV, Ostend.
20. H.S. Muralidhara, D. Ensminger and A. Putnam, 1985, Acoustic dewatering and drying (low and high frequency), *Drying Technol.*, **3**(4), 529.
21. H.S. Muralidhara, 1985, Solid-liquid separation process for fine particle suspensions by an electric and ultrasonic field, *US Patent 4561953*, December.
22. R.E. Beard and H.S. Muralidhara, 1985, Mechanistic considerations of acoustic dewatering techniques, *IEEE Ultrasonics Symposium*, pp.1072-1075.
23. H.S. Muralidhara, N. Senapati, D. Ensminger and S.P. Chauhan, 1986, Electro-acoustic separation process for fine particle suspension, *Filt. & Sep.*, **23**(6), 351.
24. K. Miyazaki, Y. Takahashi and K. Shiomi, 1988, Particle classification in a slurry with an ultrasonic filter, *Proc. Particle Technology in Relation to Filtration & Separation Conference*, pp.3.121-3.132, KIV, Antwerp.
25. E.S. Tarleton, 1988, How electric and ultrasonic fields assist membrane filtration, *Filt. & Sep.*, **25**(6), 402.
26. E.S. Tarleton and R.J. Wakeman, 1990, Microfiltration enhancement by electrical and ultrasonic force fields, *Filt. & Sep.*, **27**(3), 192.
27. A.A. Atchley and L.A. Crum, 1988, in *Ultrasound*, K.S. Suslick (Ed.), VCH Publishers, New York.
28. R.J. Urick, 1947, A sound velocity method for determining the compressibility of finely divided substances, *J. App. Phys.*, **18**, 983.
29. R.J. Urick, 1948, The absorption of sound in suspensions of irregular particles, *J. Acous. Soc. Am.*, **20**(3), 283.
30. W.S. Ament, 1953, Sound propagation in gross mixtures, *J. Acous. Soc. Am.*, **25**(4), 638.
31. J.R. Allegra and S.A. Hawley, 1971, Attenuation of sound in suspensions and emulsions: Theory and experiments, *J. Acous. Soc. Am.*, **51**(5), Pt 2, 1545.

32. A.S. Ahuja and W.R. Hendee, 1978, Effects of particle shape and orientation on propagation of sound in suspensions, *J. Acous. Soc. Am.*, **63**(4), 1074.
33. R. Rautenbach and R. Albrecht, 1989, *Membrane Processes*, Wiley, Chichester.

FIGURES AND TABLES

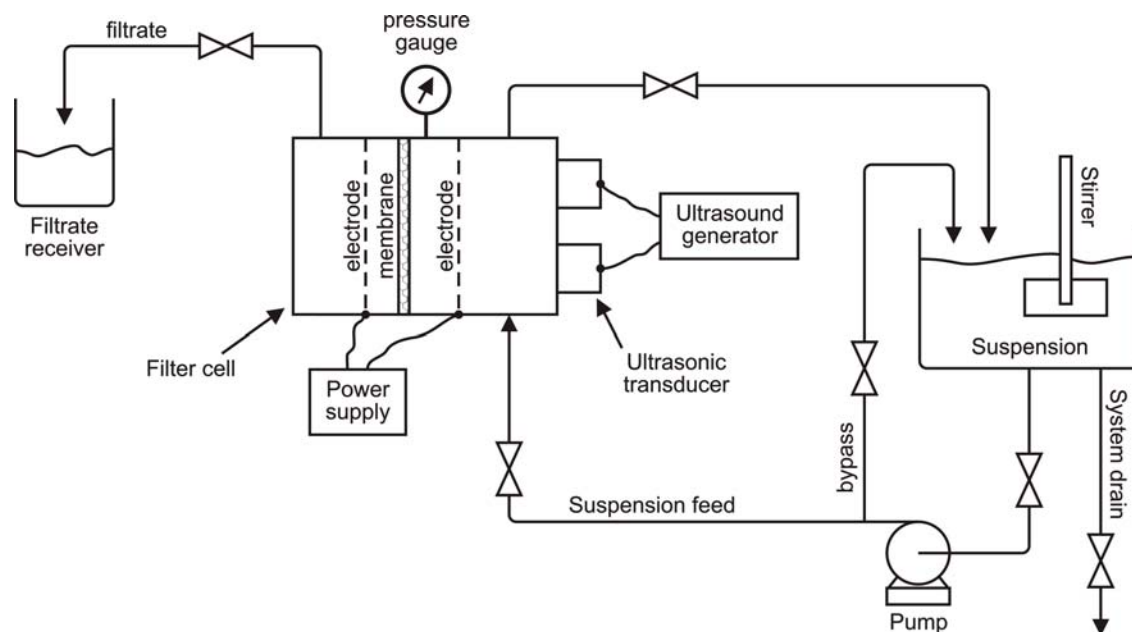


Figure 1: Schematic diagram of the experimental equipment.

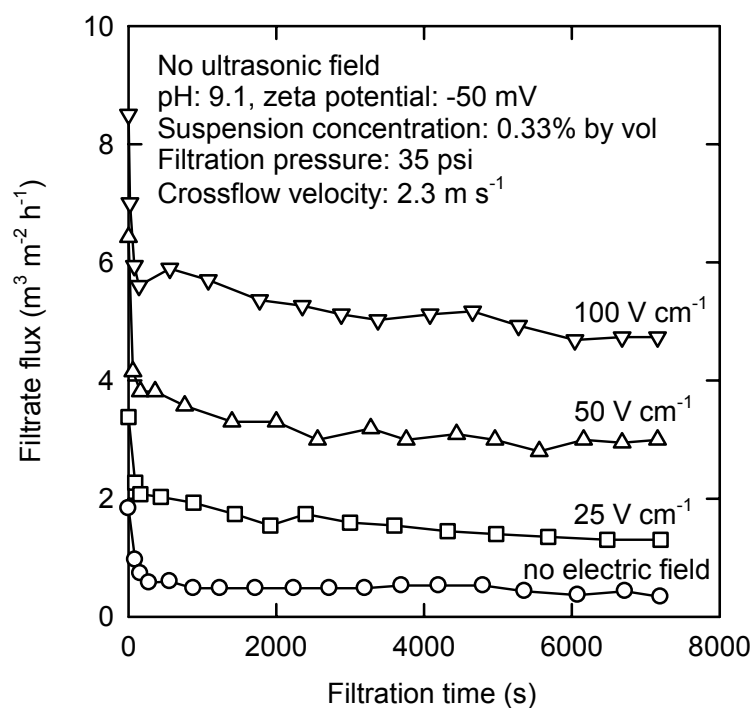


Figure 2: Effect of electric field gradient on electrically assisted filtration of anatase suspensions.

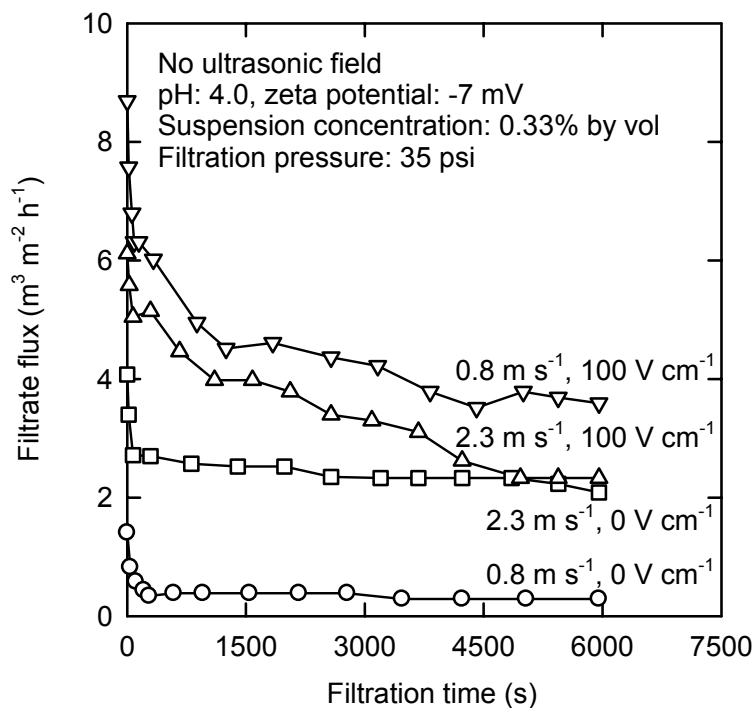


Figure 3: Effect of crossflow velocity on the filtration of anatase suspensions with and without electric fields.

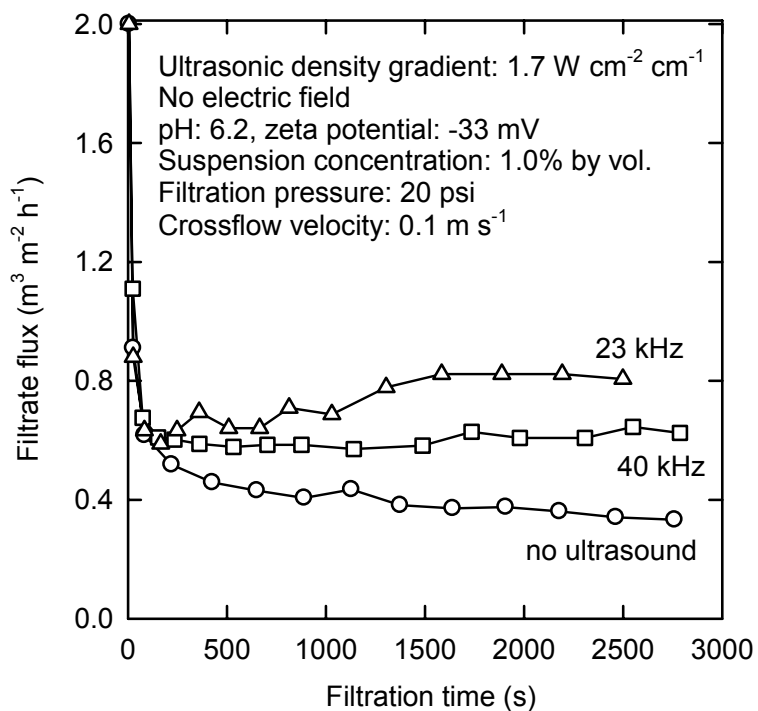


Figure 4: Effect of ultrasound frequency on ultrasonically assisted filtration of china clay suspensions.

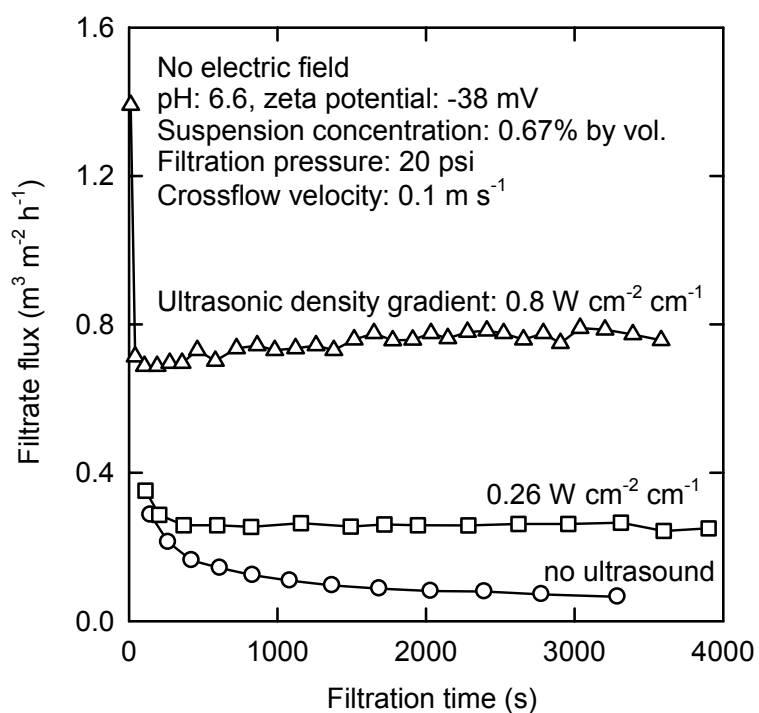


Figure 5: Effect of ultrasonic field gradient on ultrasonically assisted filtration of anatase suspensions.

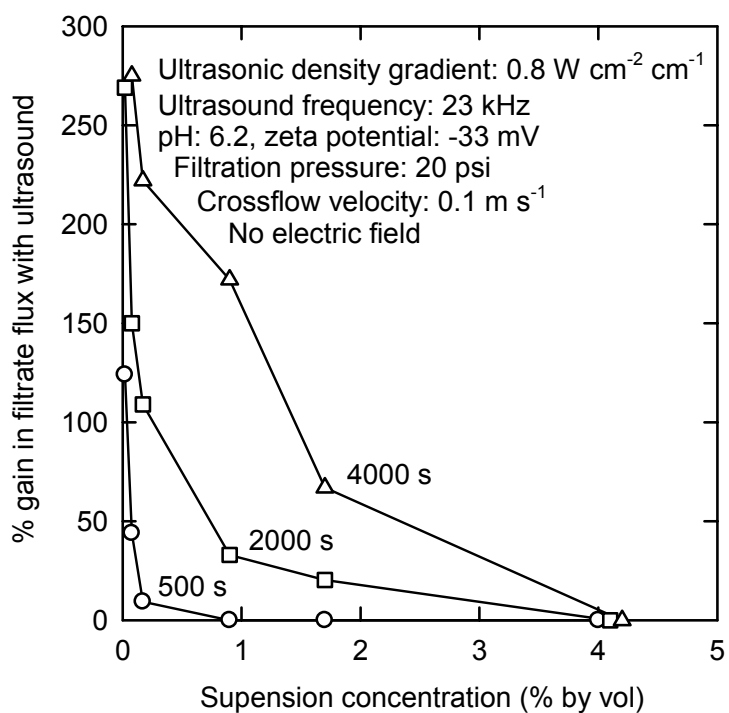


Figure 6: Effect of feed concentration on ultrasonically assisted filtration of china clay suspensions.

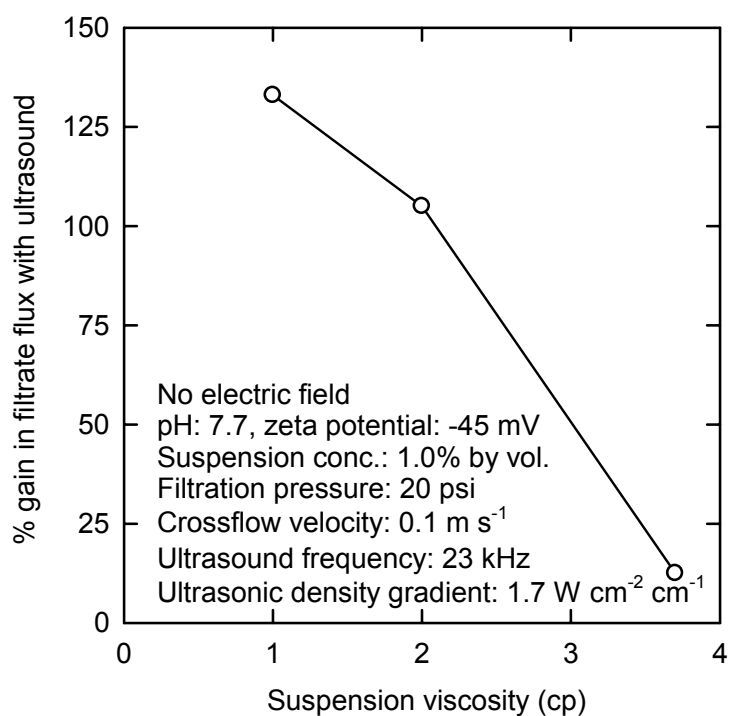


Figure 7: Effect of suspension viscosity on ultrasonically assisted filtration of china clay suspensions.

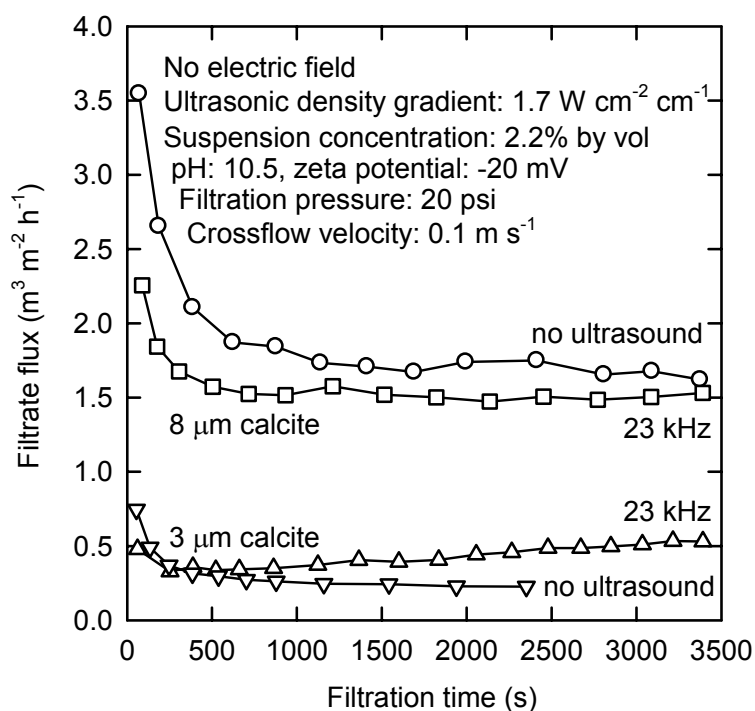


Figure 8: Effect of particle size on ultrasonically assisted filtration of calcite suspensions.

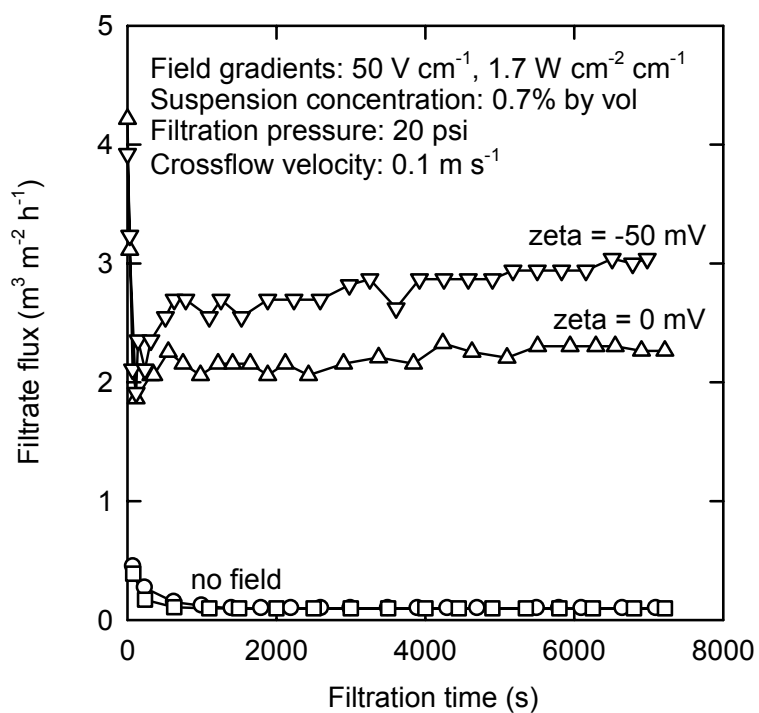


Figure 9: Effect of pH (ζ -potential) on electroacoustically assisted filtration of china clay suspensions.

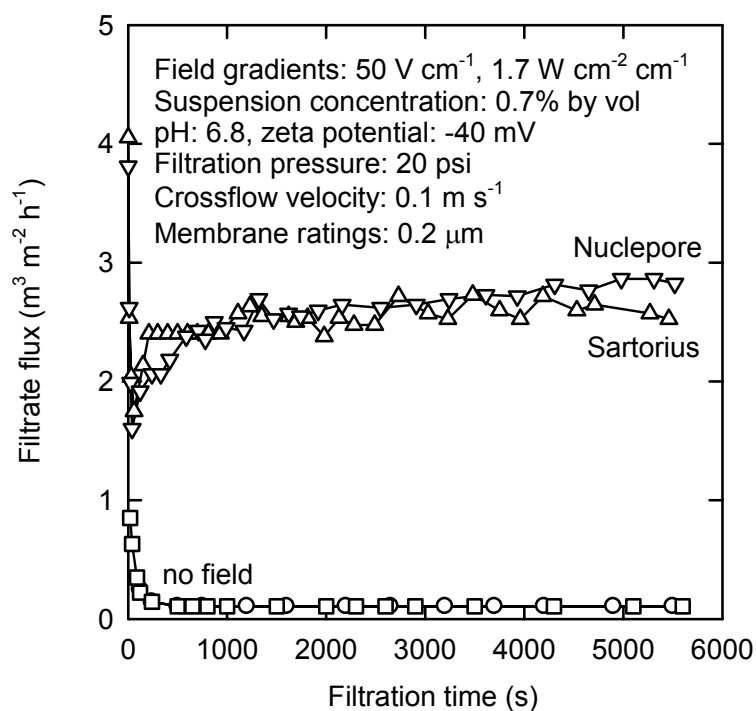


Figure 10: Effect of membrane structure on electroacoustically assisted filtration of anatase suspensions.

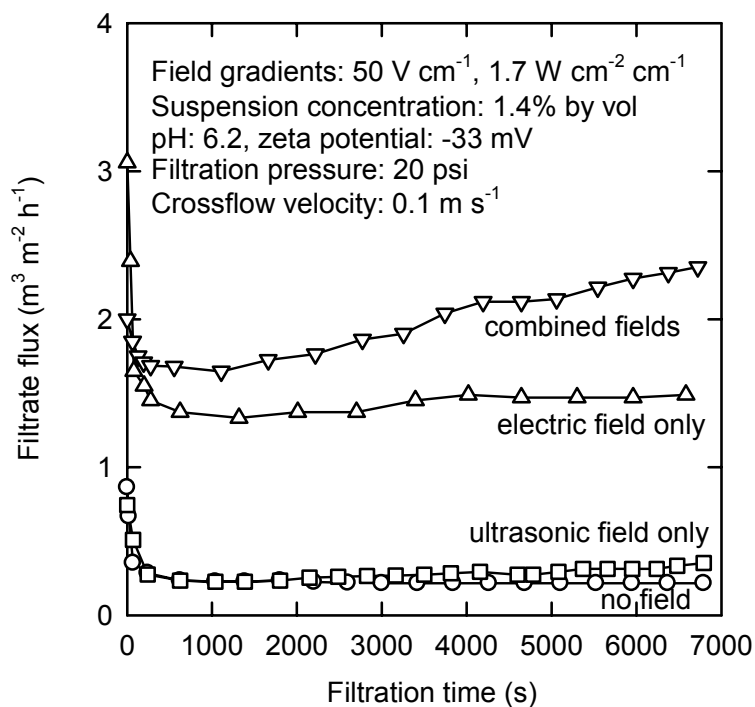


Figure 11: Synergy between electric and ultrasonic fields during the filtration of china clay suspensions.

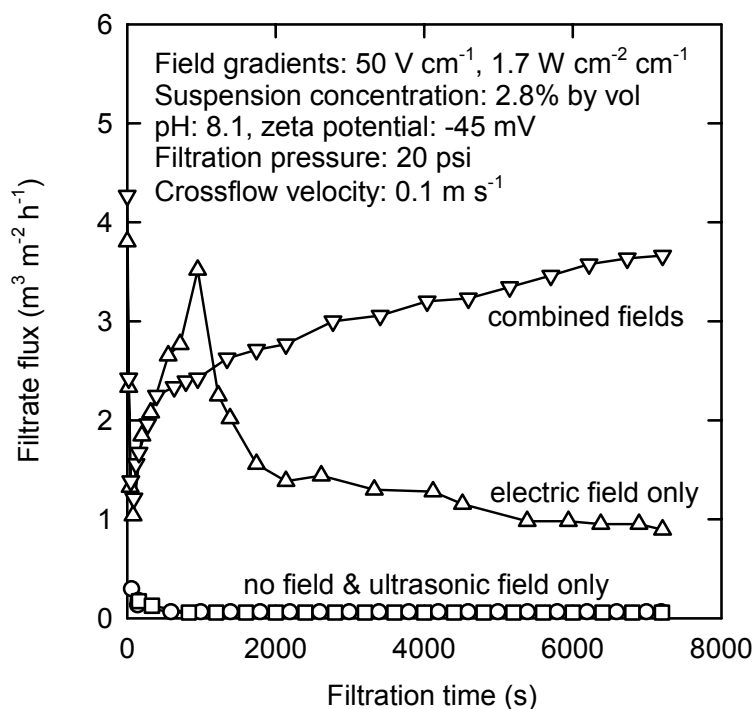


Figure 12: Synergy between electric and ultrasonic fields during the filtration of anatase suspensions.

	Anatase	Calcite	China clay
Particle size (μm)	0.5	3 and 8	3.5
Particle shape	tetragonal	rhomboidal	platelets
Zeta potential	-38 mV @ pH 6.6	-20 mV @ pH 10.5	-33 mV @ pH 6.2
Isoelectric pH	3.9	9.4	~1.2
	Asypor	Sartorius	Nuclepore
Pore rating* (μm)	0.2/0.8	0.2	0.2
Mean pore size (μm)	0.75/1.72	0.56	0.37
Pore size range (μm)	0.5-1.0/1.0-2.31	0.37-0.71	0.14-0.41

*Manufacturers designation

Table 1: Characteristics of the particles and membranes used in this work.

Feed stream	Membrane	Process parameters
Particle size pH (surface charge) Solids concentration Liquid viscosity Particle shape	Pore size Structure	Filtration pressure Crossflow velocity Electric field strength Ultrasonic field strength Ultrasonic frequency

Table 2: Matrix of properties examined in the filtration experiments.

% by volume	0.01	0.1	1	5
Anatase	0.039	0.389	3.79	17.0
Calcite	0.026	0.265	2.61	12.2
China clay	0.026	0.257	2.53	11.9

Table 3: Range of feed concentrations (% by mass) used in the experiments.

An increase of	causes a in cavitation threshold
dissolved gas saturation	decrease
hydrostatic pressure	increase
surface tension	decrease (in spite of the Laplace equation)
temperature	decrease
solids concentration	decrease
particle size	decrease
dissolved ion concentration	increase (at low concentrations)

Table 4: Parameters affecting the cavitation threshold.

Feed concentration (% v/v)	Intensity absorption coefficient, α (m^{-1})			
	China clay	Anatase	8 μm Calcite	3 μm Calcite
Frequency = 23 kHz				
0.01	0.001	0.0002	0.0024	0.0011
0.1	0.01	0.002	0.024	0.011
1	0.1	0.02	0.24	0.11
5	0.5	0.1	1.2	0.55
Frequency = 40 kHz				
0.01	0.0025	0.0004	0.0041	0.0027
0.1	0.025	0.004	0.041	0.027
1	0.25	0.04	0.41	0.27
5	1.25	0.2	2.05	1.35

Table 5: Variation of the sound intensity absorption coefficient with frequency and suspension concentration for different solids.

			Power/energy consumption*			
					Totals	
Filtrate flux ($\text{m}^3 \text{m}^{-2} \text{h}^{-1}$)	Crossflow velocity (m s^{-1})	Field gradients (V mm^{-1} $\text{W cm}^{-2} \text{cm}^{-1}$)	Applied field(s) (kW m^{-2})	Pump (kW m^{-2})	kW m^{-2}	($\text{kW h}) \text{m}^{-3}$
0.5 ^a	2.3	0	0	19.6	19.6	39.3
0.4 ^a	0.1	0	0	0.02	0.02	0.05
0.12 ^b	0.1	0	0	0.02	0.02	0.17
0.71 ^b	0.1	5	93.9	0.02	93.92	132.3
4.41 ^b	0.1	5/1.7	124.7 + 24.9	0.02	149.62	33.9
0.2 ^c	0.1	0	0	0.02	0.02	0.1
1.5 ^c	0.1	5	9.1	0.02	9.12	6.08
2.3 ^c	0.1	5/1.7	13.0 + 24.9	0.02	37.92	16.5

*Power per unit area of filter; energy per unit volume of filtrate.; ^a0.33% anatase suspension at pH 9.1; ^b2.8% anatase suspension at pH 8.1; ^c1.4% china clay suspension at pH 6.2

Table 6: Power consumptions during normal and enhanced crossflow microfiltration.

An increase of	causes a in filtration rate
Electric field strength	increase
Ultrasound frequency	decrease (best at ~23 kHz)
Ultrasonic field strength	increase
Crossflow velocity*	increase (particles < ~6 μm) decrease (particles > ~6 μm)
Particle size	decrease (upper limit ~ 6 to 8 μm)
Zeta potential	increase
Feed concentration	increase
Liquid viscosity	decrease (upper limit probably < 10 cp)

*Low velocities ~0.1 m s^{-1} can be used.

Table 7: Effect of parameters on electroacoustic filtration.